A Revised Force–Restore Model for Land Surface Modeling

DIANDONG REN AND MING XUE

School of Meteorology, and Center for Analysis and Prediction of Storms, The University of Oklahoma, Norman, Oklahoma

(Manuscript received 20 November 2002, in final form 18 May 2004)

ABSTRACT

To clarify the definition of the equation for the temperature toward which the soil skin temperature is restored, the prediction equations in the commonly used force–restore model for soil temperature are rederived from the heat conduction equation. The derivation led to a deep-layer temperature, commonly denoted T_2, that is defined as the soil temperature at depth πd plus a transient term, where d is the e-folding damping depth of soil temperature diurnal oscillations. The corresponding prediction equation for T_2 has the same form as the commonly used one except for an additional term involving the lapse rate of the ''seasonal mean'' soil temperature and the damping depth d. A term involving the same also appears in the skin temperature prediction equation, which also includes a transient term. In the literature, T_2 was initially defined as the short-term (over several days) mean of the skin temperature, but in practice it is often used as the deep-layer temperature. Such inconsistent use can lead to drift in T_2 prediction over a several-day period, as is documented in this paper. When T_2 is properly defined and initialized, large drift in T_2 prediction is avoided and the surface temperature prediction is usually improved. This is confirmed by four sets of experiments, each for a period during each season of 2000, that are initialized using and verified against measurements of the Oklahoma Atmospheric Surface-Layer Instrumentation System (OASIS) project.

1. Introduction

Land surface models (LSMs) deal with the evolution of land surface and deep soil layer conditions and the exchanges of moisture and thermal energy between the land surface and the atmosphere. Land surface modeling is important for the studies of climatic predictions (e.g., Dickinson and Henderson-Sellers 1988), hydrology (e.g., Milly and Dunne 1994), and numerical weather prediction (e.g., Betts et al. 1997; Chen and Dudhia 2001).

Among land surface models of various complexities, a so-called force–restore model for soil temperature prediction is popular (e.g., Deardorff 1978, D78 hereinafter; Noilhan and Planton 1989, NP89 hereinafter; Mahfouf et al. 1995) because of its computational efficiency and reasonable physical foundation. It employs a minimum number of prognostic variables yet captures the most important physical processes. The model was originally developed by Bhumralkar (1975, B75 hereinafter) and Blackadar (1976, B76 hereinafter), and was adopted by D78 and used in models such as the Interactions between Soil, Biosphere, and Atmosphere (ISBA; NP89; Mahfouf et al. 1995) scheme.

The force–restore model, as applied to soil temperature, usually involves two prognostic equations—one for the surface or skin temperature (T_s), representing the temperature of both canopy and soil surface, and the other for a temperature (T_2) toward which T_s is relaxed.

The definition of T_2 has not always been consistent in the literature. B75 defines it, when it appears in the equation for surface temperature, as ''the daily mean temperature at the surface assumed to be the same at all depths.'' NP89 defines it in the ISBA model in a similar way, as the mean value of T_s over 1 day. D78, however, calls it the deep soil temperature and predicts it using a different equation.

The definition of T_2 has been vague even in the same ISBA community; daily mean soil temperature is used in some papers (e.g., NP89, Mahfouf and Noilhan 1991; Noilhan and Lacarrère 1995; Noilhan and Mahfouf 1996; Calvet et al. 1998), while deep soil temperature is used in others (e.g., Bouttier et al. 1993; Boone et al. 2000). Different definitions can even be found in the same article (Bouttier et al. 1993). When T_2 is considered deep soil temperature, different depths have been used. For example, Bouttier et al. (1993) considered T_2 the temperature at a 1-m depth, while Calvet et al. (1998) and Mahfouf and Noilhan (1991) used the temperature at 0.81 m. In Mahfouf and Noilhan (1991), even though T_2 is defined as the mean daily temperature (p. 1357), measurement at a 81-cm depth is used to initialize T_2 (p. 1358). These differences in definition often lead to confusion in interpreting and verifying the model results.

Corresponding author address: Dr. Ming Xue, School of Meteorology, University of Oklahoma, 100 East Boyd, Norman, OK 73019. E-mail: mxue@ou.edu.

© 2004 American Meteorological Society

One reason for the seemingly interchangeable use of daily average temperature and the deep soil temperature may have risen from the original assumption of B75, who assumed that the daily mean temperature is the same at all depths. This assumption may be valid in the spring and autumn seasons but is certainly not true in most parts of the world during the summer and winter (de Vries 1963). Figure 1a shows the Oklahoma Atmospheric Surface-Layer Instrumentation System (OASIS; Brotzge et al. 1999) project measurements of soil temperature at ground level, and those at 25- and 60-cm depths for a 7-day summer period starting from 12 August 2000. The mean of these three temperature time series are, respectively, 306.7, 304.2, and 301.2 K, indicating a decreasing trend with depth. The difference between the mean temperatures of skin and 60 cm is as large as 5.5 K for this period. A reverse trend is apparent for the winter period (a 7-day period starting from 5 January 2000, shown in Fig. 1b), where the soil temperatures at 5, 25, and 60 cm have respective means of 280.0, 281.1, and 283.4 K. The temperature increases with depth in this case. The above behavior appears to be also observed by Mahfouf et al. (1995), who found for climate simulations a spurious drift toward too-low temperatures, especially over continental areas during polar nights. Their solution to this problem with a force–restore model is to add another term to the rhs of the T_2 equation that relaxes T_2 toward a climatological deep soil temperature. While it appears to work, the physical basis for doing so is not entirely clear.

In this study, the soil model in the Advanced Regional Prediction System (ARPS; Xue et al. 1995, 2000, 2001) is tested against OASIS-observed soil temperature data in week-long periods during four different seasons. The model is based on NP89 and some of its later modifications. Drift on the order of 5 K is found in the predicted variable T_2, when it is initialized using observed deep soil temperature. This discrepancy, along with the confusing state with the definition of T_2 and its prediction equation, motivated us to take another look at the equation. As a result, a new definition of the T_2 is obtained by rederiving the equation starting from the heat conductivity equation. The resultant prediction equation for T_2 has the same form as the one commonly used, except for an additional term involving the lapse rate of the ''seasonal mean'' soil temperature and the damping depth *d*. A term involving the same also appears in the skin temperature prediction equation, which also includes a transient term.

It is found that when T_2 is properly defined and initialized, large drift in T_2 prediction is avoided and the surface temperature prediction is usually improved. In section 2, the equations as used by B75 and NP89 are first briefly reviewed, followed by the derivation of a revised version. The physical meaning of T_2 will also be discussed. The OASIS data used in this study will be described in section 3. The design of the numerical experiments will be given in section 4, and numerical results will be presented in section 5. Conclusions are given in section 6.

2. The revised force–restore model for soil temperature

a. Prognostic equations for soil temperature and the force–restore model

The equation describing the time evolution of soil temperature T can be written in terms of the vertical flux convergence, assuming that the effect of horizontal heat exchange can be neglected:

$$C\frac{\partial T}{\partial t} = -\frac{\partial G}{\partial z}, \qquad -\infty < z \le 0, \tag{1}$$

where G is the heat flux given by the following:

$$G(z, t) = \begin{cases} G_0 & z = 0, \\ -K_T C\dfrac{\partial T}{\partial z} & z < 0. \end{cases} \tag{2}$$

Here, C is the volumetric soil heat capacity (J m^{-3} K^{-1}), t is the time, z is the vertical coordinate (positive upward and zero at the ground surface), and K_T is the soil thermal diffusivity (m^2 s^{-1}) that is related to soil thermal conductivity λ (W m^{-1} K^{-1}) by soil heat capacity, that is, $K_T = \lambda/C$. In Eq. (2), G_0 is the net heat flux at the ground given by

$$G_0 = \mathrm{LE} + H - R_n, \tag{3}$$

where R_n is the net radiation flux at the surface that includes net short- and longwave radiation, LE is the latent heat, and H is the sensible heat flux leaving the ground surface.

For the interior of the soil, Eq. (1) becomes

$$C\frac{\partial T}{\partial t} = \frac{\partial}{\partial z}\left(\lambda\frac{\partial T}{\partial z}\right). \tag{4}$$

If λ is assumed to be constant,

$$C\frac{\partial T}{\partial t} = \lambda\frac{\partial T^2}{\partial z^2}. \tag{5}$$

In the case in which the vertical variation in thermal conductivity is relatively small, a simplified model derived from Eq. (4), with λ set as constant, can be rather accurate. The force–restore model is such a model, and it was originally developed by B75 and B76 and popularized by D78. It is the basis of land surface models such as ISBA (NP89; Mahfouf et al. 1995).

In B75, the temperature at the surface is assumed to be sinusoidal with a 24-h diurnal cycle and is expressed as

$$T(0, t) = \overline{T} + A\sin(\omega t), \tag{6}$$

where ω is the frequency of oscillation ($\omega = 2\pi/\tau$, with τ being the period of oscillation equal to 24 h), $\overline{T}$ is defined as the daily average temperature of the soil that is assumed to be the same at all depths, and A is the

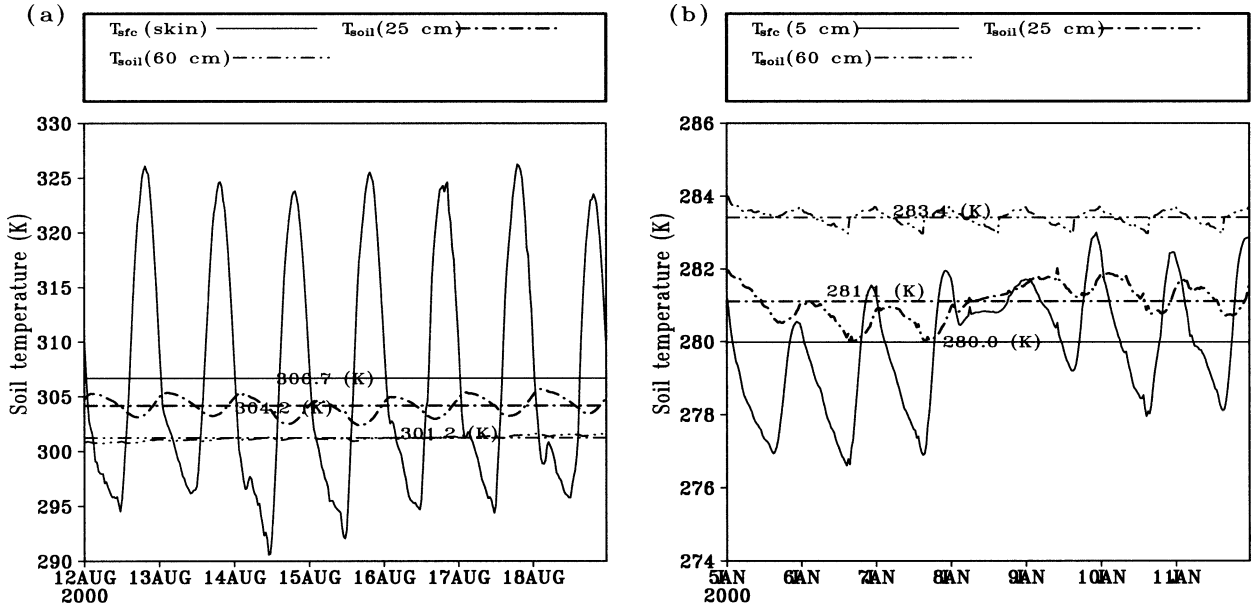

FIG. 1. OASIS-observed soil temperatures for 7-day periods starting from (a) 12 Aug and (b) 5 Jan 2000. Solid lines show soil skin temperature for the Aug case and 5-cm soil temperature for the Jan case, dot–dash lines show 25-cm temperature, and dot–dot–dash lines show 60-cm temperature. The weekly averages are shown as horizontal lines of the same styles. The values of the period mean temperatures are labeled.

amplitude of temperature wave at the surface. An equation for the mean temperature in a thin surface layer of depth d_1 (taken to be 1 cm) was obtained by B75 as follows:

$$c\frac{\partial T_s}{\partial t} = G_0 - \left(\frac{\omega C\lambda}{2}\right)^{1/2}(T_s - \overline{T}), \tag{7}$$

where T_s is the ground surface temperature, $c = d_1C + \sqrt{\lambda C/2\omega}$, and G_0 is the net surface heat flux given in Eq. (3). It is this equation, or a variation thereof, that is used in land surface models like that of NP89. In NP89, the definition of c is approximated by dropping the first term on the rhs of its definition, that is, term d_1C. This approximation actually originated from and was discussed in D78, and it is equivalent to assuming that the heat capacity of this thin layer is so small that the surface heat flux into this thin layer is roughly balanced by the ground heat flux in the deep layer.

With the above approximation or consideration, Eq. (7) becomes

$$\frac{\partial T_s}{\partial t} = C_G G_0 - \frac{2\pi}{\tau}(T_s - T_2), \tag{8}$$

where $C_G \equiv \sqrt{2\omega/\lambda C}$. When vegetation is present, this coefficient will be modified to include the effect of vegetation on heat capacity (see, e.g., NP89). In the above equation, the daily mean temperature $\overline{T}$ has been replaced by a new symbol T_2, because variable $\overline{T}$ has become a time-dependent variable to be predicted by another equation (to be discussed next). Symbol $\overline{T}$, with an overbar denoting time averaging, can be misleading. Equation (8), in a slightly different form, was also tested by D78.

In NP89, a second equation is given for $\overline{T}$, now named T_2, but still defined as the daily mean temperature:

$$\frac{\partial T_2}{\partial t} = \frac{1}{\tau}(T_s - T_2). \tag{9}$$

No detail on the derivation of this equation was, however, given in NP89, except for references to B75 and B76. Interestingly, neither B75 nor B76 provided the equation for the prediction of T_2. In B76, it is said that "the value to be used for θ_m (our T_2) is the mean temperature of the surface air during the most recent 24 hours."

As discussed in the introduction, the definition of T_2 has not always been consistent in the literature. In the following section, we rederive the two equations for soil temperature and attempt to establish a clear definition for T_2. It is hoped that this definition will also help us to avoid certain misuse of measurement data or model predictions.

b. Revised force–restore model for soil temperature

Here we define the seasonal mean soil temperature as the running mean of temperature over 1–2 weeks, a period that is long enough to remove diurnal temperature changes while retaining the seasonal variations. In general, this temperature increases (decreases) downward in winter (summer). Seasonal mean temperature can be considered the background upon which the diurnal oscillations are superimposed. This temperature is

similar to the mean temperature defined by B75 except that we do not assume it to be constant at all depths. We will see that taking into account the vertical variation in this mean temperature introduces additional terms into the force–restore equations.

Suppose this seasonal mean temperature profile of the soil is given by $\tilde{T}_z = \tilde{T}_s + \gamma z$, where $\tilde{T}_s$ is the mean temperature at the surface, and γ is the ''lapse rate'' of the mean temperature (positive as temperature decreases with depth). Thus, under sinusoidal surface forcing with single dominant period, as in the form of Eq. (6), the soil temperature as a solution to Eq. (5) can be found to be

$$T(z, t) = \tilde{T}_s + \gamma z + Ae^{z/d} \sin\left(\omega t + \phi_0 + \frac{z}{d}\right), \quad (10)$$

where $\phi_0 \equiv \omega t_0$ is the initial phase, t_0 is the time at which the amplitude of surface temperature oscillation is zero, and $d = \sqrt{K_\tau \tau/\pi} \equiv \sqrt{2\lambda/C\omega}$ is the e-folding damping depth at which the amplitude of surface temperature oscillations is reduced by a factor of e^{-1} (about 0.37). Obviously, it is a function of soil thermal diffusivity and the period of forcing. In this study as well as in B75, K_T was assumed to be constant with depth.

The general solution for soil temperature in Eq. (10) tells us that the amplitude of soil temperature fluctuations decreases exponentially with depth and the phase delay increases linearly with depth; the amplitude is dampened faster with depth for high-frequency modes, which justifies our using of only one mode (daily cycle) in the analysis.

The background soil temperature profile also implies an extra soil heat flux of constant magnitude, that is, $-\lambda\gamma$, for all depths. Thus, at the surface ($z = 0$), the soil heat flux $G(0, t) = G_0 - \lambda\gamma$, or, there is a modification to the definition of Eq. (3). When we plug the solution of T in Eq. (10) into the definition of ground heat flux in (2), we obtain

$$G(z, t) = -\lambda\left\{\gamma + \frac{1}{d}Ae^{z/d}\left[\sin\left(\omega t + \phi_0 + \frac{z}{d}\right) + \cos\left(\omega t + \phi_0 + \frac{z}{d}\right)\right]\right\}. \quad (11)$$

From Eq. (10) and its time derivative we have

$$Ae^{z/d} \sin\left(\omega t + \phi_0 + \frac{z}{d}\right) = T(z, t) - \tilde{T}_s - \gamma z \quad (12)$$

and

$$Ae^{z/d} \cos\left(\omega t + \phi_0 + \frac{z}{d}\right) = \frac{1}{\omega}\frac{\partial T(z, t)}{\partial t}. \quad (13)$$

In obtaining Eq. (13), we have assumed that γ is a very slowly varying function of time; therefore, its time derivative can be neglected. Plugging Eqs. (12) and (13) into Eq. (11), we obtain

$$G(z, t) = -\lambda\left\{\gamma + \frac{1}{d}\left[T(z, t) - \tilde{T}_s - \gamma z + \frac{1}{\omega}\frac{\partial T(z, t)}{\partial t}\right]\right\}. \quad (14)$$

Applying Eq. (14) to $z = 0$, and making use of the surface energy balance [Eq. (3)], we obtain, after some reorganization,

$$\frac{\partial T(0, t)}{\partial t} = \frac{2\pi}{\tau}[\tilde{T}_s - T(0, t)] + \frac{d\omega}{\lambda}(R_{\text{net}} - \text{LE} - H), \quad (15)$$

where $(d\omega)/\lambda \approx 1/c$. If we designate $C_G \equiv 1/c \approx 2/(dC)$, Eq. (15) can be rewritten as

$$\frac{\partial T(0, t)}{\partial t} = C_G(R_{\text{net}} - \text{LE} - H) + \frac{2\pi}{\tau}[\tilde{T}_s - T(0, t)]. \quad (16)$$

Equation (16) is essentially the force–restore equation for surface temperature derived by B75 and used in models of D78 and NP89. The key issue here is the definition of the temperature toward which the surface temperature is restored. In Eq. (16), this temperature is $\tilde{T}_s$, the temporal mean surface temperature.

In Eq. (16) $\tilde{T}_s$, defined as the time-mean surface temperature, is not known. It is a slow-varying quantity and we choose to relate it to a temperature of the deep-layer soil of some sort. Here we set out to derive an equation for the mean (vertically averaged) temperature of the deep layer. The mean temperature of the layer extending from the ground level to a depth at z is defined by $\overline{T}_2 \equiv 1/z \int_0^z T(z', t)\, dz'$. Plugging in $T(z)$ given by Eq. (10) gives

$$\overline{T}_2 = \tilde{T}_s + \frac{\gamma z}{2} + \frac{dA}{2z}e^{z/d}\left[\sin\left(\omega t + \phi_0 + \frac{z}{d}\right) - \cos\left(\omega t + \phi_0 + \frac{z}{d}\right)\right] - \frac{dA}{2z}[\sin(\omega t + \phi_0) - \cos(\omega t + \phi_0)]. \quad (17)$$

Taking a time derivative of Eq. (17) and making use of Eq. (12), we have

$$\frac{\partial \overline{T}_2}{\partial t} = \frac{d\omega}{2z}\left\{Ae^{z/d}\left[\sin\left(\omega t + \phi_0 + \frac{z}{d}\right) - \sin(\omega t + \phi_0)\right] + [T(z, t) - T(0, t) - \gamma z]\right\}. \quad (18)$$

Letting $z = -\pi d$, that is, choosing the depth of the layer for which we look for the vertical mean to be πd, Eq. (18) becomes

$$\frac{\partial \overline{T_{(0\sim -\pi d)}}}{\partial t} = \frac{A\omega}{2\pi}(e^{-\pi} + 1)\cos(\omega t + \phi_0) - \frac{1}{\tau}[T(-\pi d, t) - T(0, t) + \gamma \pi d]. \quad (19)$$

Let $z = -\pi d$, and again we obtain the mean temperature in the πd deep layer as

$$\overline{T_{(0\sim -\pi d)}} = \tilde{T}_s - \frac{\gamma \pi d}{2} + \frac{A(1 + e^{-\pi})}{2\pi} \times [\sin(\omega t + \phi_0) - \cos(\omega t + \phi_0)]. \quad (20)$$

Applying Eq. (12) at $z = -\pi d$ and rearranging, we have

$$\tilde{T}_s = T(-\pi d, t) + Ae^{-\pi}\sin(\omega t + \phi_0) + \gamma \pi d. \quad (21)$$

After plugging the above equation into Eq. (20), we obtain

$$\overline{T_{(0\sim -\pi d)}} = T(-\pi d, t) + \frac{\gamma \pi d}{2} + A\left[e^{-\pi} + \frac{(1 + e^{-\pi})}{2\pi}\right]\sin(\omega t + \phi_0) - \frac{A(1 + e^{-\pi})}{2\pi}\cos(\omega t + \phi_0). \quad (22)$$

Let

$$\overline{T_{(0\sim -\pi d)}} = T^{(1)} + \frac{\pi d}{2}\gamma + \frac{A}{2\pi}(e^{-\pi} + 1)\sin(\omega t + \phi_0), \quad (23)$$

where

$$T^{(1)} = T(-\pi d, t) - \frac{A(1 + e^{-\pi})}{2\pi}\cos(\omega t + \phi_0) + Ae^{-\pi}\sin(\omega t + \phi_0) = T(-\pi d, t) + AB\sin(\omega t + \phi_0 + \alpha),$$

$$\alpha = \tan^{-1}\left[\frac{-(1 + e^{-\pi})}{2\pi e^{-\pi}}\right] \approx -0.42\pi, \quad \text{and}$$

$$B = \left[\left(\frac{1 + e^{-\pi}}{2\pi}\right)^2 + e^{-2\pi}\right]^{0.5} \approx 0.17. \quad (24)$$

By plugging $\overline{T_{(0\sim -\pi d)}}$ given in Eq. (23) into Eq. (19), making use of Eq. (13) applied at $z = 0$, we obtain

$$\frac{\partial T^{(1)}}{\partial t} = -\frac{1}{\tau}[T(-\pi d, t) - T(0, t) + \gamma \pi d] = -\frac{1}{\tau}[T^{(1)} - T(0, t) + \gamma \pi d] + \frac{AB}{\tau}\sin(\omega t + \phi_0 + \alpha). \quad (25)$$

Equation (25) is similar to the deep-layer temperature equation used in traditional force–restore models (e.g., NP89), except for the sine term on the rhs and the $\gamma \pi d$ term. The sine term considerably complicates the equation. We want to see if the equation can be simplified through further variable transformation. We define $T^{(1)} = T^{(2)} - (AB/2\pi)\cos(\omega t + \phi_0 + \alpha)$ and plug it into Eq. (25) to obtain

$$\frac{\partial T^{(2)}}{\partial t} = -\frac{1}{\tau}[T^{(2)} - T(0, t) + \gamma \pi d] + \frac{AB}{2\pi\tau}\cos(\omega t + \phi_0 + \alpha). \quad (26)$$

Equation (26) is more attractive than Eq. (25) because the last term on the rhs is a factor of 2π smaller than that in Eq. (25). The next transform would be $T^{(2)} = T^{(3)} + (AB/2\pi)^2\sin(\omega t + \phi_0 + \alpha)$, and Eq. (26) can then be rewritten as

$$\frac{\partial T^{(3)}}{\partial t} = -\frac{1}{\tau}[T^{(3)} - T(0, t) + \gamma \pi d] - \frac{AB}{(2\pi)^2\tau}\sin(\omega t + \phi_0 + \alpha), \quad (27)$$

whose last term on the rhs is yet another factor of 2π smaller! The next transformation

$$T^{(3)} = T^{(4)} + \frac{AB}{(2\pi)^3}\cos(\omega t + \phi_0 + \alpha)$$

yields

$$\frac{\partial T^{(4)}}{\partial t} = -\frac{1}{\tau}[T^{(3)} - T(0, t) + \gamma \pi d] - \frac{AB}{(2\pi)^3\tau}\cos(\omega t + \phi_0 + \alpha). \quad (28)$$

We notice that a pattern has emerged with both the transformation and the second term on the rhs of the prognostic equation. The following general transformation can be applied:

$$T^{(2n)} = T^{(2n+1)} - (-1)^n\frac{AB}{(2\pi)^{2n}}\sin(\omega t + \phi_0 + \alpha),$$

$$T^{(2n+1)} = T^{(2n+2)} - (-1)^n\frac{AB}{(2\pi)^{2n+1}}\cos(\omega t + \phi_0 + \alpha), \quad n \geq 0,$$

where integer n is the transformation order, with $T^{(0)} = T(-\pi d, t)$.

Applying this transformation indefinitely results in the magnitude of the sinusoidal term on the rhs of the equation eventually approaching the limit of zero. At this limit, the variable that is predicted by the equation becomes

$$T_2 = T^{(\infty)} = T(-\pi d, t) + AB\left[\sum_{n=0}^{\infty}\left(\frac{-1}{4\pi^2}\right)^n\right]$$

TABLE 1. General information of Norman super-OASIS site.

Site identifier	Location	Elev (m)	Slope (°)	Land use	Soil type
NORM	35.26°N, 97.48°W	360.0	0.0	Scrub	Silty clay

$$\times \left[\sin(\omega t + \phi_0 + \alpha) + \frac{1}{2\pi}\cos(\omega t + \phi_0 + \alpha)\right]$$

$$= T(-\pi d, t) + AB\frac{4\pi^2}{4\pi^2 + 1} \times \left[\sin(\omega t + \phi_0 + \alpha) + \frac{1}{2\pi}\cos(\omega t + \phi_0 + \alpha)\right]$$

$$= T(-\pi d, t) + AB' \sin(\omega t + \phi_0 + \alpha'), \quad (29)$$

where $B' = 2\pi/(\sqrt{4\pi^2 + 1})B \approx 0.17$, $\alpha' = \alpha + \tan^{-1}(1/2\pi) \approx -0.37\pi$, and we give variable $T^{(\infty)}$ the name T_2 to match the name used for the deep-layer temperature in Eq. (9). The prognostic equation for T_2 is, therefore,

$$\frac{\partial T_2}{\partial t} = -\frac{1}{\tau}(T_2 - T_s + \gamma\pi d), \quad (30)$$

which is the same as Eq. (9), except for the term related to mean lapse rate γ. Here, we renamed $T(0, t)$ as T_s to be consistent with earlier notations in Eqs. (8) and (9).

Now, we go back to the prediction equation [Eq. (16)] for surface temperature T_s and replace $\tilde{T}_s$ in the equation with the following:

$$\tilde{T}_s = T(-\pi d, t) + \pi d\gamma + Ae^{-\pi}\sin(\omega t + \phi_0)$$

$$= T_2 + \pi d\gamma - AB' \sin(\omega t + \phi_0 + \alpha') + Ae^{-\pi}\sin(\omega t + \phi_0)$$

$$= T_2 + \pi d\gamma + AB'' \sin(\omega t + \phi_0 + \alpha''), \quad (31)$$

where $\alpha'' = \tan^{-1}[(AB' \sin\alpha')/(AB' \cos\alpha' - Ae^{-\pi})] \approx 0.45\pi$ and $B'' = \sqrt{(e^{-\pi} - B' \cos\alpha')^2 + (B' \sin\alpha')^2} \approx 0.158$, so that

$$\frac{\partial T_s}{\partial t} = C_G(R_{\text{net}} - \text{LE} - H) - \frac{2\pi}{\tau}(T_s - T_2 - \pi d\gamma) - \frac{2\pi}{\tau}AB'' \sin(\omega t + \phi_0 + \alpha''). \quad (32)$$

Equations (30) and (32) are the new force–restore equations that we obtained for predicting the deep-layer and surface soil temperatures. One of the advantages over the original force–restore equations is the clear definition of T_2 and a rigorously derived prediction equation for it. The main differences of these equations from those of NP89 include the extra $\pi d\gamma$ terms in both equations, which we will show through verification experiments against the OASIS data to be the most significant aspect of improvement with this new set of equations. The last term in Eq. (32) is a troublesome term, because the amplitude of diurnal cycle A is not known a priori. Fortunately, experiments show that the neglect of this term has little impact on the solution; in practice, it can be neglected or estimated based on the mean amplitude of the previous days.

3. OASIS data at Norman site and the use of data

This study make use of the OASIS data from the Norman, Oklahoma, site that was also used by Brotzge and Weber (2002) for soil model calibrations. The OASIS sites are part of the Oklahoma Mesonet (Brock et al. 1995) that have routine measurements of the surface energy budget. Because of high initial and maintenance costs, only 10 of the 90 OASIS sites are equipped with sonic anemometers. These 10 sites are called supersites, and the site at Norman (station named NORM) is one of them. At supersites, all components of the surface energy budget are directly measured by instruments. The Norman site is flat, and its immediate surroundings can be considered as uniform on a scale of several thousands of meters at an elevation of 360 m. The parameters used for characterizing the land surface are summarized in Table 1.

At the Norman site, routine meteorological measurements include the surface temperature, mixing ratio, precipitation rate, wind, and surface pressure. An infrared sensor records surface skin temperature. The raw data of surface meteorological variables and soil skin temperature are recorded at 5-min intervals. The measurements of soil moisture and soil temperature are made using the 229-L sensors every 0.5 h at 0.05, 0.25, 0.60, and 0.75 m from the surface downward. Because our focus here is on the soil temperature prediction, time-interpolated observed values of soil moisture (or depth-mean values) are used to specify both near-surface and deep-layer soil moisture in our validation experiments; therefore, only soil temperature is predicted by the model. The soil moisture measurements at 0.05 m are directly used to specify the near–surface layer soil moisture, and soil moisture measurements at 0.25, 0.6, and 0.75 m are weighted by their representing soil depths (i.e., 10, 30, 40, and 70 cm) to come up with a mean value for the deep soil moisture content. The soil temperature measurements at 0.05 and 0.25 m are processed according to Eq. (29) to arrive at values of T_2, which are then used to initialize as well as to verify the revised force–restore model.

All four components of the surface energy balance, that is, net radiation, sensible heat flux, latent heat flux, and ground heat flux, are directly measured every 5 min

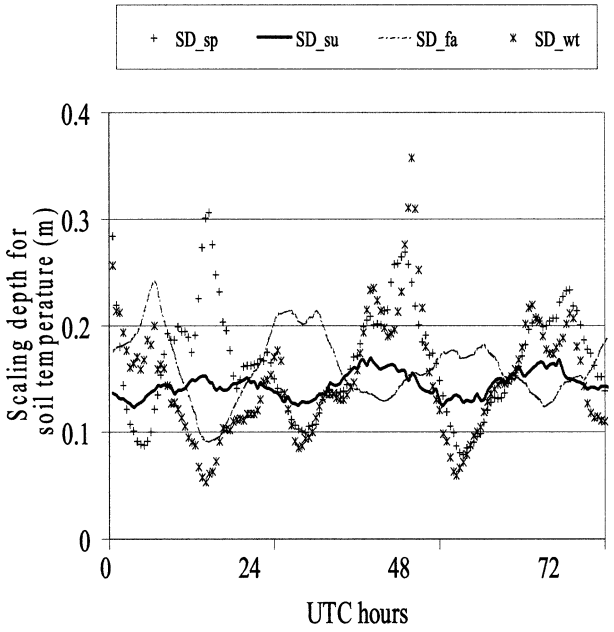

FIG. 2. Example damping depths (SD) for soil temperature calculated using the amplitude–phase method. The damping depths are calculated from soil temperatures at 5- and 25-cm depths. The starting point are 24 Mar (cross), 12 Aug (thick solid), 17 Sep (dot dash), and 9 Jan (star) for selected period in spring, summer, autumn, and winter seasons, respectively. The amplitude–phase method worked the best for the 12 Aug 2000 period.

and are available for the whole study period (Brotzge 2000). The measured radiation fluxes are used to force the soil model in our experiments (to be discussed later). The vegetation parameters recorded by OASIS include vegetation type, leaf area index (LAI), vegetation cover, and the normalized difference vegetation index (NVDI). This study involves four 6-day periods selected from each season of the year 2000. The vegetation properties are kept constant within each forecasting period.

Because T_2 is now defined as a composite value by Eq. (29), its initialization and verification should also use the same definition. Preprocessing of the deep soil temperature is performed first. In the equation, the most important factor is the determination of the damping depth of the soil temperature. The generalized amplitude–phase method (Sellers 1965, 134–139) is used to determine the damping depth (see the appendix) for each testing period because of its soil moisture dependency. This method uses the soil temperature information of two different depths at four equally separated times of a clear day. Given the data availability, the amplitude–phase method can be applied to the soil temperature measurement pairs at 5 and 25, 5 and 60, or 25 and 60 cm, to obtain three different values of the damping depth. The final optimally estimated damping depth is obtained by taking a weighted average of all three, with the first measurement pair being given the largest weight of 0.6 and the remaining two given the same weight of 0.2. Because the assumption of sinusoidal diurnal oscillations can be violated in the real soil temperature data at times, the calculated damping depth can be enormously large at these times, causing some spikes in the curves as shown in Fig. 2. Values larger than 30 cm are considered bad and are discarded. The remaining values are then averaged over each period to obtain the mean values. It was found that the mean damping depth could vary between 12 and 17 cm at the Norman site, mainly depending on the moisture content. For our four selected periods, the mean values are 0.155, 0.148, 0.164, and 0.146 m for spring, summer, fall, and winter periods, respectively, as given in the last column of Table 2.

Amplitude A in Eq. (10), by definition, is the temperature amplitude at the land surface. When the infrared sensor–measured skin temperature is generally good, skin temperature amplitude is calculated daily, and the average amplitude over the 6-day period is used. The infrared sensor measurements of skin temperature are more problem prone in the winter, due to various calibration problems as documented by Fiebrich et al. (2003). When this measurement is not good, we estimate the surface soil temperature by extrapolation from the temperature measured at a 5-cm depth using the exponential decaying relation described by Eq. (10).

In Eq. (29) T_2 includes soil temperature at depth $-\pi d$ and a sinusoidal part. For every damping depth we determined, the depth of $-\pi d$, in general, does not happen to be at one of the four fixed measurement depths of 5, 25, 60, and 75 cm. Using the method for determining the damping depth, soil temperature at $z = -\pi d$ can be derived from measurements at any available depth, that is, at 5, 25 (in this study), or 60 cm. Aside from the aforementioned amplitude A, the sinusoidal term in Eq. (29) includes an initial phase ϕ_0. This parameter signifies physically the phase delay of surface soil temperature to surface forcing and is obtained in this study by a comparison of the maximum surface soil temperature occurrence time and the time of maximum net radiation.

TABLE 2. LAI, difference between seasonal mean surface and deep-layer temperature ($\pi d\gamma$), observed period average amplitude of skin temperature (A_0) and of deep-layer temperature (A_{deep}), and damping scale depth (d) in the four study periods.

	LAI	$\pi d\gamma$ (K)	A_0 (K)	A_{deep} (K)	d (m)
Spring (25–31 Mar)	0.22	2.0	9.62	0.74	0.155
Summer (12–18 Aug)	0.60	4.70	15.52	1.34	0.148
Autumn (17–23 Sep)	0.50	−0.51	12.50	1.23	0.164
Winter (5–11 Jan)	0.06	−2.17	2.87	0.61	0.146

4. Numerical model and experimental design

The implementation of the two-layer soil–vegetation model in ARPS basically follows the ISBA model (NP89) with some of its later enhancements. In the model, the surface layer depth is set as 0.1 m and the deep layer is assumed to be at 1 m deep. The deep soil layer acts as a reservoir for heat as well as for soil water.

The amplitude of daily soil temperature cycle depends highly on the volumetric heat capacity of the combined ground–vegetation surface layer, while the volumetric heat capacity for ground in ISBA depends on both soil texture and the wetness of the soil at the time. The heat capacity of vegetation is set as 2×10^{-5} K m^2 J^{-1} at NORM. The volumetric heat capacity also determines the relative importance of surface forcing (energy balance) term and the restore term in surface temperature equation. According to NP89, for the Norman site (with slope of logarithmic water retention curve $b = 10.4$), the soil heat capacity can vary by a factor of 7 between that when soil moisture content is near saturation ($w_{\text{sat}} = 0.45$ m^3 m^{-3}) and that at wilting point (heat capacity is 3.729×10^{-6} K m^2 J^{-1} when $w_{\text{with}} = 0.19$ m^3 m^{-3}).

Because our primary goal is to evaluate the performance of the soil model, in our experiments, we run the soil model in a stand-alone forced mode to avoid uncertainties due to atmospheric processes. Shortwave (solar) radiation reaching the ground (which is needed in the parameterization of evapotranspiration process), net radiation, wind speed (at 2 m AGL), surface pressure, air temperature (2 m AGL), and specific humidity (2 m AGL) are all specified using OASIS measurements that are linearly interpolated to the model time steps where they are needed. The time step size used for the land surface model is 1 min. The surface latent heat and sensible heat fluxes are calculated using the stability-dependent surface flux model in the ARPS, instead of using those from OASIS measurements. Doing so permits the feedback of surface soil temperature and moisture prediction to the surface energy balance through surface flux calculations.

To match the height (2 m AGL) at which the meteorological measurements are taken, a stretched vertical grid with a minimum grid spacing of 4 m at the ground is used so that the first model level for temperature, moisture, and horizontal is 2 m AGL (because of grid staggering). The remaining parameters, including the leaf area index, soil type, surface roughness, minimum stomatal resistance, and vegetation cover are specified according to the properties of the Norman site (see Tables 1 and 2 for some of the parameter values). The vegetation cover and surface roughness data provided by OASIS is not *seasonally varying*, and values of 0.75 and 0.03 m, respectively, are used following Brotzge and Weber (2002). The soil texture–related parameters are specified for silty clay soil types according to Table 2 of NP89. The minimum stomatal resistance is set as 200 s m^{-1}, and the threshold solar radiation strength for shutting down transpiration at dust is 50 W m^{-2}.

Four different groups of experiments are performed for each season, and they are termed "*original*," "*lapse rate only*," "*sine term only*," and "*revised*," respectively, based on the formulation of the equations used. By lapse rate only we mean that the only modification to the original formulation is to take into account the difference between the average temperatures of the top and deep layers, that is, to include the $\pi d\gamma$ terms in the restoring terms in the rhs of Eqs. (30) and (32). By sine-term only we mean that the modification is only limited to the sinusoidal term introduced in Eq. (32). By revised we mean that we fully implemented the terms in Eqs. (30) and (32). All results are compared with properly processed OASIS measurements (denoted observation in the figures). For T_2, this means that Eq. (29) (with and without the transient term, depending the run) is used to determine its observed value. Such values are also used to initialize T_2 at the initial time. Because the sine term is not easy to determine in advance in practical applications, we want to see if its inclusion in the equations is significant. Last, as mentioned earlier, soil moisture content is specified according to OASIS observations. Comparison runs with predicted soil moisture show similar results, however.

To examine the effects of the modifications to the force–restore equations, in particular, the inclusion of the seasonal mean temperature lapse rate terms, four periods of 6 days each from four different seasons in year 2000 were selected. They are as follows: 25–31 March (from spring), 12–18 August (from summer), 17–23 September (from early autumn), and 5–11 January (from winter). In selecting the study periods, top priority is given to the coherency among the soil and atmospheric measurements. Quiescent, high pressure–dominated clear-sky conditions are preferred to have more periodic surface forcing. Figure 3 shows, using the summer season as an example, regular periodic behavior in both fluxes at the surface and in the temperature of air and soil. Figure 3a exhibits the periodic daily cycles of various measured energy fluxes. Figure 3b shows that, under such periodic forcing, both surface skin temperature and the soil temperatures at 5 cm show periodic diurnal cycles of evolution.

The selected winter is different from the other three periods in two aspects. This period is wetter (superficial soil moisture content $w_g = 0.379$ m^3 m^{-3}, and deep soil moisture content $w_2 = 0.384$ m^3 m^{-3}) than the other periods ($w_g = 0.25$ m^3 m^{-3} and $w_2 = 0.270$ m^3 m^{-3} for summer; $w_g = 0.24$ m^3 m^{-3} and $w_2 = 0.269$ m^3 m^{-3} for autumn; $w_g = 0.36$ m^3 m^{-3} and $w_2 = 0.38$ m^3 m^{-3} for spring). This fact is reflected in the damping depth (Table 2), which is shallower for the winter. As mentioned in section 3, during much of the winter season, the infrared sensor measurements are contaminated. For 5–11 January 2000, the surface soil temperatures are obtained by extrapolation from the temperature mea-

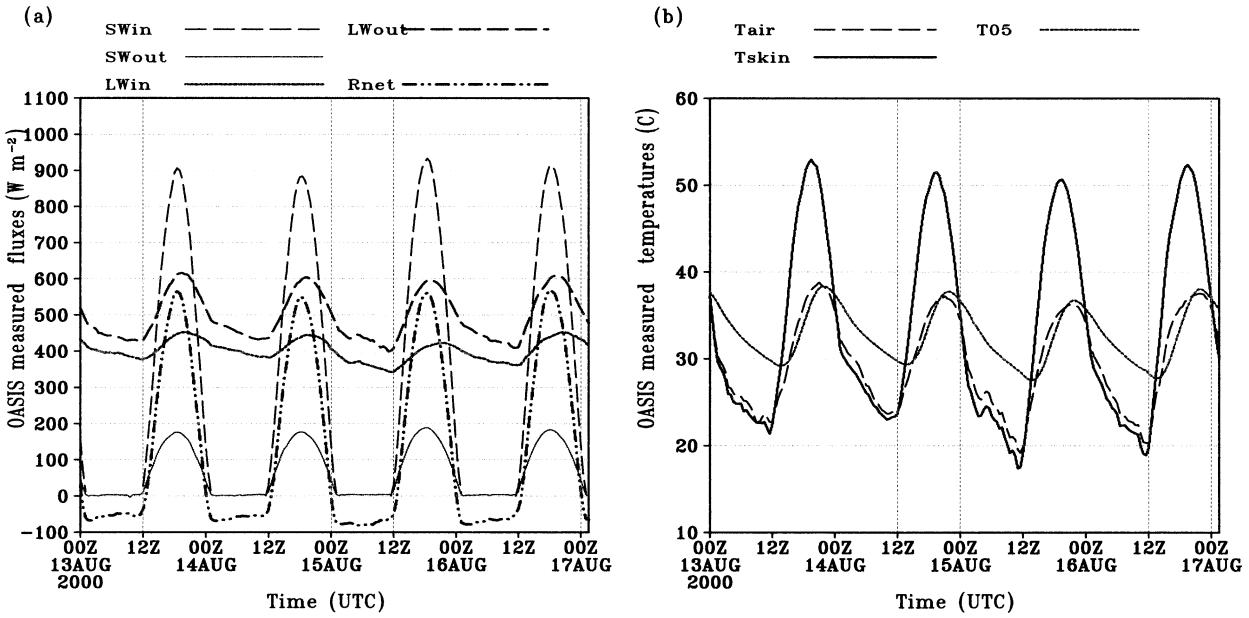

FIG. 3. OASIS measurements for the period of 13–17 Aug 2000. (a) SWin is incoming shortwave flux, SWout is reflected shortwave flux, LWout means outgoing longwave radiation, LWin means downward longwave radiation, and Rnet is the net radiation; (b) T_{air} is air temperature at 2 m, T_{skin} is skin temperature measured by the infrared instrument, and T05 is soil temperature at 5-cm depth.

sured at a 5-cm depth using the exponential decaying relation described by Eq. (10).

5. Results of experiments

We present in this section results of the numerical experiments outlined earlier. We first look at the results from the 6-day summer period starting from 12 August 2000. Figure 4 shows model-predicted and observed skin and deep soil temperature T_s and T_2, respectively, for this period using different formulations. The surface temperature forecasts, by either the original or modified formulations, are most accurate for the first 2 days; those for the rest of the period are also fairly accurate (Fig. 4a). The root-mean-square error is 1.5 K for the entire period. No apparent phase error exists, and the amplitude difference is generally less than 3 K. The maximum amplitude errors occur mainly at the time of maximum daytime heating, and a maximum difference of 3.86 K occurred at around 1700 UTC 14 August 2000. There exists a general, though small, cold bias in the skin temperature forecast of about -0.58 K, as indicated by both minimum and maximum daily temperatures.

The deep soil temperature predicted by the original formulation has large errors (Fig. 4b); the rms error is 3.32 K for the 6-day period (Table 3). The predicted values are consistently 4–5 K higher than the observed ones only one-half day from the initial time, although the diurnal oscillations are generally in phase with the observations. A careful look indicates that there is a tendency for the daily mean value of T_2 to approach the daily mean of T_s, a result, we believe, caused primarily by the neglect of mean lapse rate of the soil temperature, which is 4.7 K over a 46-cm depth (see Table 2). Note that here T_2 is initialized in all cases according to Eq. (29), which represents soil temperature as certain depth. If T_2 is initialized for the original formulation at some form of mean surface temperature, the drift noted above is expected to be much smaller. However, in most published papers, T_2 is initialized using estimated or measured deep soil temperature (e.g., Mahfouf and Noilhan 1991; Bouttier et al. 1993; Pleim and Xiu 1995; Noilhan and Mahfouf 1996; Xiu and Pleim 2001).

The T_2 predictions using revised and lapse rate–only formulations are much closer to those observed (Fig. 4b). The rms error is about 0.7 K in both runs, and the reduction is mainly due to the removal of the upward drift observed in the original case. The figure also shows that the inclusion of the sine term made very little difference from the original solution, and the solutions of revised and lapse rate–only cases are also very close. This indicates that the inclusion of the sine term in both cases has very little impact. Because of the difficulty with knowing the amplitude of surface oscillations a priori, the sine or transient terms in our derived equations can be safely neglected in practice. As shown in Table 3, the revised formulation consistently gives a better T_2 forecast in all four seasons, and the difference is most dramatic in the summer and winter.

The inclusion of the lapse rate–related term in the skin temperature prediction equation [i.e., Eq. (32)] did not affect the already rather accurate prediction of skin temperature much in this case. The slight cold bias in the skin temperature still exists (Fig. 4a). This must be because in the skin temperature equation, the forcing

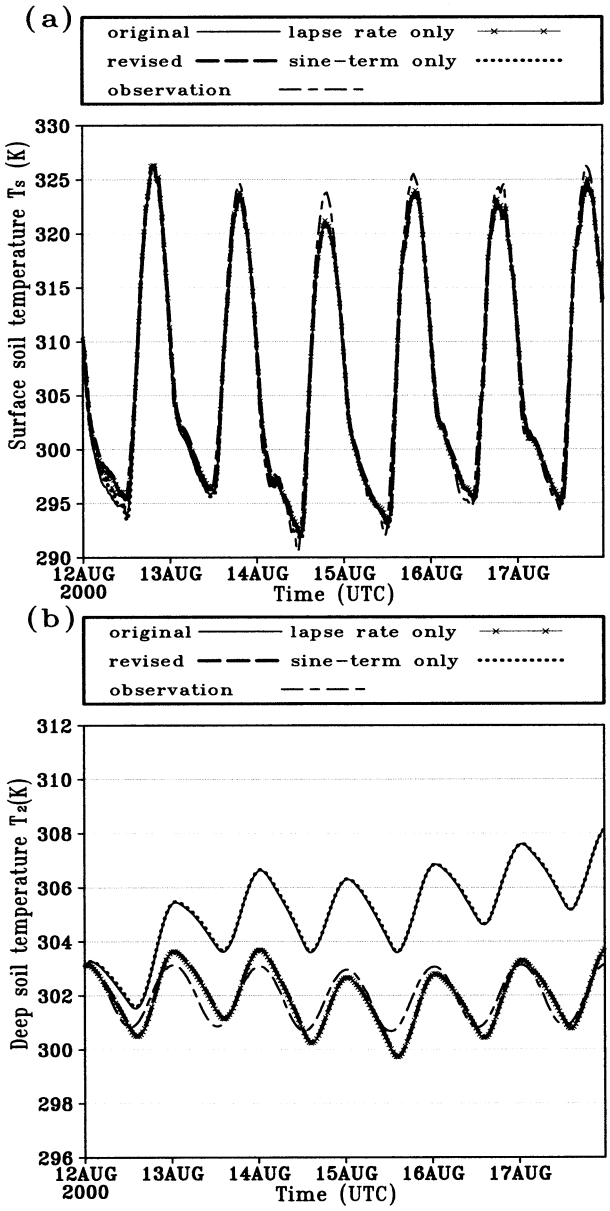

FIG. 4. Model-predicted and observed (a) surface and (b) deep soil temperatures for a 6-day summer period, starting from 0000 UTC 12 Aug 2000, using different versions of the force–restore model. The thin solid line is for the original force–restore model (original case), thin solid line with cross markers is for the lapse rate–only case (see text for definition), the dotted line without marker refers to the sine term–only case, and the long dashed line refers to the case with a complete implementation of our modifications to the force–restore model, the revised case. The long–short dash line is for OASIS measurements.

from the net radiation and sensible heat fluxes plays a much larger role than the extra restore terms we added. The net radiative flux is, especially during the daytime heating period, the dominant term. We noted earlier that there is little phase delay in our skin temperature prediction, but a problem was reported by Brotzge and Weber (2002) in tests with 1 day in May and 2 days in August of the same year using the same model and dataset. This improvement can be shown to be due to better behavior of the soil moisture, which in our case is specified according to observations. Improvements to the ARPS soil moisture prediction equations have been made since the work of Brotzge and Weber (2002) by the current authors, and the predicted soil moisture content is now much closer to the observed values; as a result, tests using predicted soil moisture now produce very similar temperature forecasts.

The results from the 6-day winter period starting from 0000 UTC 5 January 2000 are presented in Fig. 5. As pointed out earlier, the observed skin temperature in this case is extrapolated from the soil temperature measured at 5 cm using Eq. (10). In general, the revised model, or the version that includes the lapse rate–related terms, provides a better deep soil temperature forecast (Fig. 5b). In this case, the T_2 predicted by the original formulation has a tendency to drift below the temperature of the observed values, opposite in direction to the summer case. This can again be explained by the fact that the mean lapse rate is neglected in the original formulation and in winter the mean surface temperature is lower than the mean temperature at the deeper layer. The original model tends to pull the deep-layer temperature toward that of the surface. The improvement in T_2 forecast is not as consistent through the period as in the summer, however. This can be attributed to the fact that during this period, the surface temperature is not very periodic from day 4 (8 January 2000). The first 3 days represent a clear, calm period after a cold-frontal passage, whereas the last 2 days are a warming-up period. For day 4, the observed shortwave solar radiation fluxes reaching the ground clearly indicate cloudy sky conditions, and the daily maximum downward longwave radiation shows a 30% increase that prevented surface temperature from decreasing as much at night. The aperiodic behavior in the skin temperature leads to poorer prediction of both skin and deep-layer temperatures from day 4 to day 5.

In contrast to the selected summer period, the daytime forcing is milder in the winter. Also, soil moisture content is larger because of several antecedent rainfall events (with the most recent one occurring on 3 January). Estimated using the soil moisture content at 5 cm, the volumetric soil heat capacity of this winter period is 2.6 times that of the summer period. This effect works in accord with the reduced energy balance term and significantly reduces the relative importance of the $C_G(R_{\text{net}} - \text{LE} - H)$ term in Eq. (32). Using the same error statistics, Table 4 illustrates the effect of our modifications on the surface temperature prediction. The rms error for surface temperature with the revised version is reduced to 0.73 from 1.06 K. The mean bias error is also significantly reduced from 0.85 to 0.34 K. Similar results were found when we applied the same modifications to another wet period starting from 0000 UTC

TABLE 3. Error statistics of T_2 predictions for different formulations and periods.

Period and mean T_2	Formulation	Rms (K)	Mean bias error (K)	Max absolute error (K)
	Original	3.3246	3.1323	5.00
Summer	Revised	0.6839	−0.3237	1.89
$\overline{T_2}$ = 301.98	Lapse rate only	0.7019	−0.3699	1.96
	Sine term only	3.3772	3.1866	5.12
	Original	1.439	−1.282	2.69
Winter	Revised	0.920	0.10	1.58
$\overline{T_2}$ = 282.52	Lapse rate only	0.895	0.14	1.57
	Sine term only	1.434	−1.268	2.73
	Original	1.086	−0.64	3.50
Autumn	Revised	1.043	0.43	2.60
$\overline{T_2}$ = 298.59	Lapse rate only	1.029	0.39	2.59
	Sine term only	1.074	−0.60	3.50
	Original	2.20	1.739	3.87
Spring	Revised	1.54	0.062	3.09
$\overline{T_2}$ = 286.98	Lapse rate only	1.55	0.021	3.14
	Sine term only	2.24	1.783	3.93

6 April 2000, suggesting that our revised formulation also improves the forecast of surface temperature and the effect is more evident when the primary force term in the equation is weaker.

The results from the 6-day early autumn period starting from 17 September 2000 are shown in Fig. 6. The daily minimum skin temperature is well predicted, with the difference from the observation being less than 2 K for all of the days. The model fails to produce similarly high daytime maximum temperatures as those observed for all of the days, although the difference is generally less than 5 K (except for day 4 when the maximum skin temperature is significantly lower than the other days). This abrupt change in the atmospheric forcing must have contributed to this larger error because interruption of sinusoidal behavior of surface conditions is expected to increase errors in force–restore model prediction. The predictions of the deep-layer soil temperature using the revised or lapse rate–only version of the model are generally better than those of the original or the sine term–only case, except for day 4 (20 September), when the surface temperature exhibited nonsinusoidal behavior (Fig. 6b). The original deep soil temperature curve drifts downward and then oscillates around a level that is about 0.6 K colder than the observed mean deep soil temperature. After including the lapse rate–related terms, the T_2 curve oscillates around a value closer to the true mean value of the deep soil temperature, giving a much closer fit to the observations. A more careful look shows that in the first 0.5 day, the difference between the modified and the original version is small, but the difference grows larger with time and reaches a steady level after two days. This is so because the restore term in the original formulation acts to drag the deep-layer temperature toward the mean surface temperature, which is about 298.6 K, instead of the seasonal mean temperature of 299.2 K (in this case). Again, the inclusion of the lapse rate terms is most effective in improving the deep soil temperature prediction and the effect of including the sine terms is negligible; these results are consistent with those of earlier cases.

For the spring of 2000, it was hard to find a week-long period with totally clear sky conditions at the Norman site. For the 25–31 March period, the first 4 days generally satisfy the periodic atmospheric forcing conditions at the surface. At day 5, there was a cold-frontal passage that caused a significant daytime temperature drop (Fig. 7a). Our calculation obtains the average soil temperatures using data from all 6 days, resulting in a smaller average temperature difference between the surface and deep layer. This explains at least partly why the deep soil temperature trend is not totally removed for the first 4 days of simulation (Fig. 7b) when the atmospheric forcing is rather periodic. Still, with the inclusion of the lapse rate term, the deep-layer temperature error is reduced by about half (Fig. 7b and Table 3), or 2°–3° most of the time. The improvement in the skin temperature forecast is evident (see Table 3), though not as large. It should be noted that the skin temperature forecast is not bad (rms $\approx$ 1.5 K and maximum absolute error $\approx$ 3 K for the revised model), despite the nonperiodic behavior around day 4.

To avoid the interference of the cold-frontal passage in the later part of the period, we repeated the test using data from the first 3 days only, for which the mean temperature difference between the surface and the deep layer is 3.5 instead of 2 K. In this case, the revised scheme gives a much-improved deep soil temperature forecast (figures not shown). The differences between the forecast and observations are within 1 K, and no apparent phase error is found. The original formulation has a maximum error of more than 2 K. Note that because there is a difference in the *e*-folding scaling depth in the two cases, T_2 is not defined at exactly the same depth.

The numerical experiments for all four seasons share the commonality that when T_2 is considered the deep soil temperature and initialized as such, the most effec-

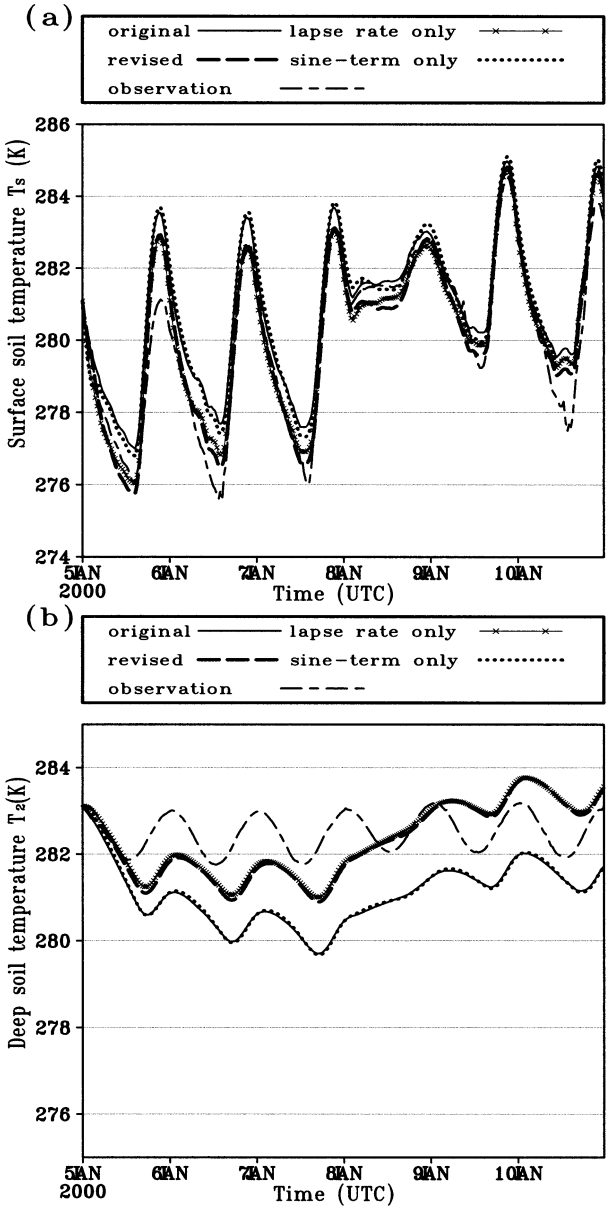

FIG. 5. As in Fig. 4, but for the 6-day winter period starting from 0000 UTC 5 Jan 2000.

tive factor for avoiding the drift in the T_2 forecast is to include the effect of seasonal mean temperature lapse rate in the equations. The sine terms are of minimal significance and can, therefore, be neglected. The improvement to the skin temperature by the revised formulation is evident, though not as dramatic.

6. Summary and conclusions

In an attempt to clarify the definition and to improve the forecast of the temperature toward which the soil skin temperature is restored in a force–restore model, we rederived the equations starting from the funda-

TABLE 4. Error statistics of T_s predictions with different formulations for the winter period.

Winter $\overline{T_s}$ = 280.352	Rms (K)	Mean bias error (K)	Max absolute error (K)
Original	1.06	0.85	2.53
Revised	0.73	0.34	2.33
Lapse rate only	0.77	0.36	2.40
Sine term only	1.04	0.84	2.63

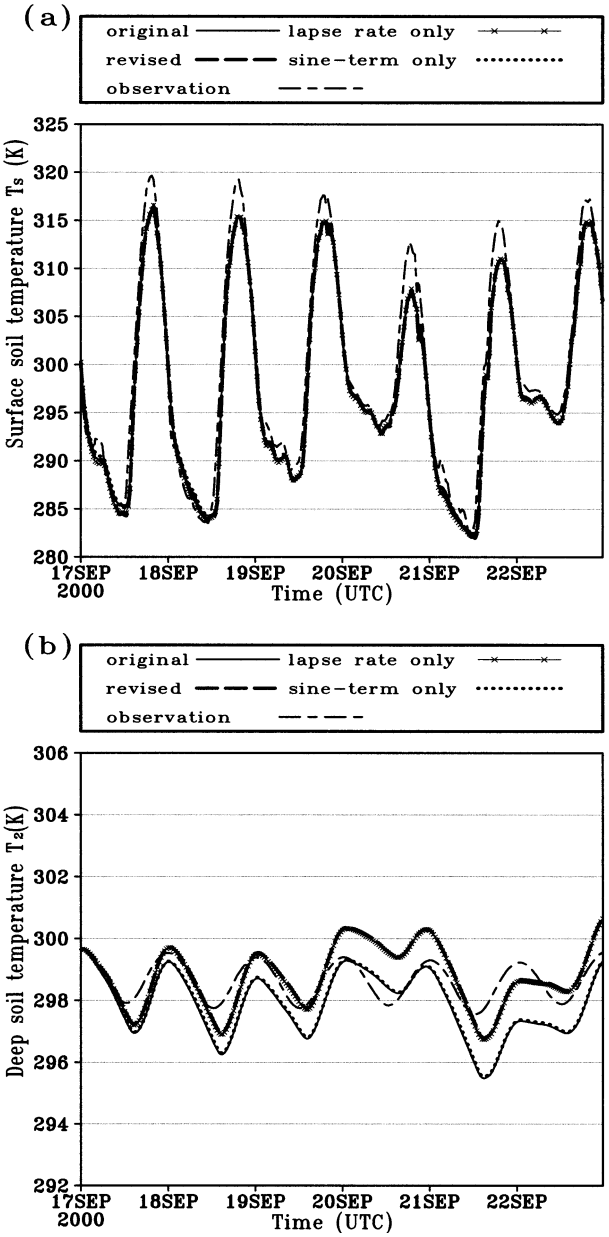

FIG. 6. As in Fig. 4, but for the 6-day early autumn period starting from 0000 UTC 17 Sep 2000.

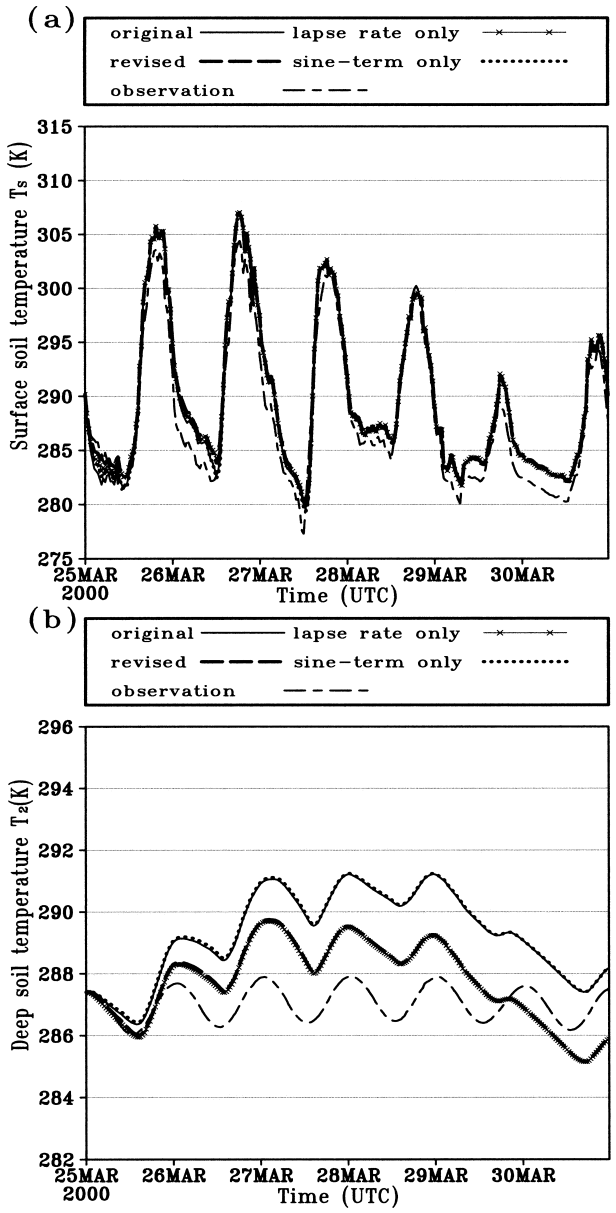

FIG. 7. As in Fig. 4, but for the 6-day spring period starting from 0000 UTC 25 Mar 2000.

mental heat conduction equation. Our derivation led to a ''deep layer'' temperature, commonly denoted as T_2, that is defined as the soil temperature at depth πd plus a transient term, where d is the e-folding damping depth of soil temperature diurnal oscillations [c.f. Eq. (29)]. Corresponding to this new definition, the prediction equation for T_2, Eq. (30), has the same form as the commonly used one (e.g., NP79), except for an additional term involving the lapse rate of the ''seasonal mean'' soil temperature and the damping depth d. A term involving the same also appears in the skin temperature prediction equation, Eq. (32), which also includes a transient term. The impact on the soil temperature prediction by these additional terms is tested against OASIS observations for four week-long periods selected out of four different seasons in 2000.

The results from these experiments show clear improvement in the prediction by our revised formulation of both skin and deep-layer temperatures with the improvement in the latter being much more dramatic. The inclusion of the transient (sine) terms and the lapse rate–related terms is tested separately. It is found that the most effective modification that improves the deep soil temperature forecast is the one that takes into account the seasonal mean soil temperature lapse rate. The inclusion of the transient (sine) terms is of minimal impact; therefore, the transient terms in both the definition of T_2 and the skin temperature equation can be neglected without much impact. The recommended equations to use are Eqs. (32), (30), and (29) with terms involving sine neglected.

It was found that without the inclusion of the $\pi d\gamma$ terms, the deep-layer temperature, when initialized as such, would drift from observed initial value toward the mean of skin temperature, and such drift was found to be on the order of 5 K for winter and summer for the Norman site, while it is of opposite sign in winter and summer. The inclusion of $\pi d\gamma$ terms virtually removes such a drift. We note here that as hard as we have searched the literature, we did not find a rigorous derivation of an equation for the prediction of T_2. Presenting a clean definition of T_2 and its prediction equation is one of the main contributions of this paper.

For dry conditions and periods with relatively strong daytime heating, our revision does not affect the skin temperature forecast as much, but the improvement becomes more significant for wetter periods. The value of our revision is further supported by the results of our recent work in which the improved force–restore model, together with equations for soil moisture, is used to build an adjoint-based four-dimensional variational data assimilation (4DVAR) system for retrieving initial conditions of the soil model (Ren and Xue 2004). The retrieval of the initial soil temperature and moisture is much better with the revised formulation.

We note here that if we keep the original formulation of the force–restore model and define and initialize T_2 as the mean of skin temperature, the drift we observed would be much smaller. The key problem is that the T_2 used here is commonly considered the deep-layer temperature (see references cited earlier), and properly predicted deep soil temperature is or can be used in parameterizing vegetation processes that involve deep roots. For this reason, there is clear value in having the deep-layer temperature available. This will be more relevant when the land surface scheme is used in coupled mode with the atmospheric components, because there will be more feedback from the calculations of heat and moisture fluxes, including that from evapotranspiration.

To use the revised system, one does need to determine $\pi\gamma d$ first. Here, $\pi\gamma d$ is the difference between the sea-

sonal mean skin and deep-layer temperature, with the latter defined at depth πd. For NWP applications that range from a few hours to two weeks, these two values can be estimated from data of the proceeding days, given that deep-layer soil moisture, a quantity that affects d most, is slowly varying. The data can be either observed or model forecast values, with the former being preferred. For longer-term applications, climatological values are suggested. Because the needed values are seasonal means, the use of climatological values is not as bad as it may sound. Parameter d can be determined by the amplitude–phase method, as is done in this paper.

Acknowledgments. This work was supported by DOT-FAA Grant NA17RJ1227-01, and NSF Grants ATM9909007 and ATM0129892. The authors thank Dr. Jerry Brotzge for making available the OASIS dataset and for very helpful discussions on related issues.

APPENDIX

The Amplitude–Phase Method for Determining *e*-Folding Damping Depth of Soil Temperature

Suppose four observations are taken regularly during each day, at 6-h intervals at two different depths; it is straightforward to get the following estimate for soil thermal diffusivity (Sellers 1965):

$$K_T = \frac{4\pi(d_2 - d_1)^2}{\tau} \times \left\{ \ln \frac{[T_1(d_1) - T_3(d_1)]^2 + [T_2(d_1) - T_4(d_1)]^2}{[T_1(d_2) - T_3(d_2)]^2 + [T_2(d_2) - T_4(d_2)]^2} \right\}^{-2},$$

where d_1 and d_2 are two different depths, τ is period of daily cycle (i.e., 86 400 s), and T_1, T_2, T_3, and T_4 are temperature measurements at 0000, 0600, 1200, and 1800 UTC, respectively. The e-folding damping depth can then be calculated according to $d = \sqrt{K_T \tau/\pi}$.

This method works better for clear-sky conditions. Also, to have a better result, d_1 and d_2 should be separated as far as possible but all within the damping depth d. Because daily oscillations cannot penetrate beyond 60 cm for normal soils, it is suggested that the two selected depths should all be limited to within the 60-cm depth.

For example, on 25 March 2000, from OASIS measurements at NORM, 5-cm soil temperatures at 0000, 0600, 1200, and 1800 UTC are 292.52, 290.28, 288.61, and 289.90 K, respectively, and 25-cm soil temperatures are 288.83, 289.30, 289.08, and 288.40 K, respectively. Using the formula, one obtains $K_T = 7 \times 10^{-7}$ m^2 s^{-1}. Thus, $d = 13.87$ cm, and $\pi d = 43.6$ cm. Soil temperature damping depths for the four seasons are obtained by applying this method to each day and then taking the average.

REFERENCES

Betts, A. K., F. Chen, K. E. Mitchell, and Z. I. Janji, 1997: Assessment of the land surface and boundary layer models in two operational versions of the NCEP Eta Model using FIFE data. *Mon. Wea. Rev.*, **125,** 2896–2916.

Bhumralkar, C. M., 1975: Numerical experiments on the computation of ground surface temperature in an atmospheric general circulation model. *J. Appl. Meteor.*, **14,** 1246–1258.

Blackadar, A. K., 1976: Modeling the nocturnal boundary layer. *Proc. Third Symp. on Atmospheric Turbulence Diffusion and Air Quality,* Boston, MA, Amer. Meteor. Soc., 46–49.

Boone, A., V. Masson, T. Meyers, and J. Noilhan, 2000: The influence of the inclusion of soil freezing on simulations by a Soil-Vegetation-Atmosphere Transfer scheme. *J. Appl. Meteor.,* **39,** 1544–1569.

Bouttier, F., J.-F. Mahfouf, and J. Noilhan, 1993: Sequential assimilation of soil moisture from low-level atmospheric parameters. Part I: Sensitivity and calibration studies. *J. Appl. Meteor.,* **32,** 1335–1351.

Brock, F. V., K. C. Crawford, R. L. Elliott, G. W. Cuperus, S. J. Stadler, H. L. Johnson, and M. D. Eilts, 1995: The Oklahoma Mesonet: A technical overview. *J. Atmos. Oceanic Technol.,* **12,** 5–19.

Brotzge, J. A., 2000: Closure of the surface energy budget. Ph.D. dissertation, University of Oklahoma, 208 pp.

——, and D. Weber, 2002: Land-surface scheme validation using the Oklahoma atmospheric surface-layer instrumentation system (OASIS) and Oklahoma Mesonet data: Preliminary results. *Meteor. Atmos. Phys.,* **80,** 189–206.

——, S. J. Richardson, K. C. Crawford, T. W. Horst, F. V. Brock, K. S. Humes, Z. Sorbjan, and R. L. Elliott, 1999: The Oklahoma Atmospheric Surface-Layer Instrumentation System (OASIS) project. Preprints, *13th Conf. on Boundary Layers and Turbulence,* Dallas, TX, Amer. Meteor. Soc., 612–615.

Calvet, J.-C., J. Noilhan, and P. Bessemoulin, 1998: Retrieving the root-zone soil moisture from surface soil moisture or temperature estimates: A feasibility study based on field measurements. *J. Appl. Meteor.,* **37,** 371–386.

Chen, F., and J. Dudhia, 2001: Coupling an advanced land surface–hydrology model with the Penn State-NCAR MM5 modeling system. Part I: Model implementation and sensitivity. *Mon. Wea. Rev.,* **129,** 569–585.

Deardorff, J. W., 1978: Efficient prediction of ground surface temperature and moisture, with inclusion of a layer of vegetation. *J. Geophys. Res.,* **83** (C4), 1889–1903.

de Vries, D. A., 1963: Thermal properties of soils. *Physics of Plant Environment,* W. R. V. Wijk, Ed., John Wiley and Sons, 210–235.

Dickinson, R. E., and A. Henderson-Sellers, 1988: Modelling tropical deforestation: A study of GCM land-surface parametrizations. *Quart. J. Roy. Meteor. Soc.,* **114,** 439–462.

Fiebrich, C. A., J. E. Martinez, J. A. Brotzge, and J. B. Basara, 2003: The Oklahoma Mesonet's skin temperature network. *J. Atmos. Oceanic Technol.,* **20,** 1496–1504.

Mahfouf, J. F., and J. Noilhan, 1991: Comparative study of various formulations of evaporation from bare soil using in situ data. *J. Appl. Meteor.,* **30,** 1354–1365.

——, A. O. Manzi, J. Noilhan, H. Giordani, and M. Deque, 1995: The land surface scheme ISBA within the Meteo-France climate model ARPEGE. Part I: Implementation and preliminary results. *J. Climate,* **8,** 2039–2057.

Milly, P. C. D., and K. A. Dunne, 1994: Sensitivity of the global water cycle to the water-holding capacity of land. *J. Climate,* **7,** 506–526.

Noilhan, J., and S. Planton, 1989: A simple parameterization of land surface processes for meteorological models. *Mon. Wea. Rev.,* **117,** 536–549.

——, and P. Lacarrère, 1995: GCM grid-scale evaporation from mesoscale modeling. *J. Climate,* **8,** 206–223.

——, and ——, 1996: The ISBA land surface parameterization scheme. *Global Planet. Change,* **13,** 145–159.

Pleim, J. E., and A. Xiu, 1995: Development and testing of a surface flux and planetary boundary layer model for application in mesoscale models. *J. Appl. Meteor.,* **34,** 16–32.

Ren, D., and M. Xue, 2004: 4DVAR assimilation of ground temperature for the estimation of soil moisture and temperature. *Extended Abstracts, 20th Conf. on Weather Analysis and Forecasting/16th Conf. on Numerical Weather Prediction,* Seattle, WA, Amer. Meteor. Soc., CD-ROM, 22.1.

Sellers, W. D., 1965: *Physical Climatology.* University of Chicago Press, 272 pp.

Xiu, A., and J. E. Pleim, 2001: Development of a land surface model. Part I: Application in a mesoscale meteorological model. *J. Appl. Meteor.,* **40,** 192–209.

Xue, M., K. K. Droegemeier, V. Wong, A. Shapiro, and K. Brewster, 1995: ARPS version 4.0 user's guide. 380 pp. [Available online at http://www.caps.ou.edu/ARPS.]

——, ——, and ——, 2000: The Advanced Regional Prediction System (ARPS)—A multiscale nonhydrostatic atmospheric simulation and prediction tool. Part I: Model dynamics and verification. *Meteor. Atmos. Phys.,* **75,** 161–193.

——, and Coauthors, 2001: The Advanced Regional Prediction System (ARPS)—A multiscale nonhydrostatic atmospheric simulation and prediction tool. Part II: Model physics and applications. *Meteor. Atmos. Phys.,* **76,** 143–165.